Menoufia J. of Electronic Engineering Research (MJEER), Vol. 32 , No. 1, ,2023

Effects of Solar Irradiance and Temperature on Photovoltaic Module Characteristics using a capacitive load method

Eman sayed ward
Department of Physics
Egyptian Academy For Engineering & Advanced Technology
Cairo, Egypt
Eman.sayed@eaeat-academy.edu.eg
(ORCID: 0000-0002-5573-463x)

Nasr Gad
Department of Physics
Ain Shams University, Faculty of Science
Cairo, Egypt
ngad@sci.asu.edu.eg
(ORCID: 0000-0002-4175-877X)

M.Lotfy Rabeh
Electrical Department
Faculty of Engineering, Shoubra, Benha University
Cairo, Egypt
mohamed.lotffi@feng.bu.edu.eg
(ORCID: 0000-0002-1254-3067)

Ashraf Yahia
Department of Physics
Ain Shams University, Faculty of Science
Cairo, Egypt
ayahia@sci.asu.edu.eg
(ORCID: 0000-0003-1998-4647)

***Abstract*— The electrical performance of photovoltaic (PV) cells or arrays is greatly influenced by the ambient temperature and the solar radiation intensity (irradiation) as well. The effect of temperature and solar irradiance on the main characteristics of solar panels and photovoltaic modules is investigated in this paper. The primary parameters are identified and extracted using the capacitive load approach. These parameters are Short Circuit Current (I_{sc}), Maximum Power Point Current (I_{mpp}), Open Circuit Voltage (V_{oc}), Maximum Power Point Voltage (V_{mpp}), Maximum Power Point (P_{max}), Fill factor (FF) and Efficiency (η). The PV cell used in this study is poly-crystal silicon. Its commercial name is Kyocera solar KC130GT. MATLAB Simulink is used to assess the capacitive load method in the investigation of I-V and P-V curves. These two curves are derived based on the effects of varying temperatures (30, 35, 40, and 45°C) at a constant irradiance (1000 W/m^2) on the PV cell performance and the effect of varying irradiance (250, 500, 750, and 1000 W/m^2) at constant temperature (25°C) as well. It is concluded that by increasing the irradiance at constant temperature, I_{sc} and V_{oc} are increasing. As a result, η increases from 13.9% at 250 W/m^2 to reach 14.7% at 1000 W/m^2. In the case of increasing temperature at constant irradiance, η decreases from 13.5% at 30°C to reach 12.8% at 45°C. This is due to the large drop in V_{oc} compared to the small increment in I_{sc}.**

Keywords*— I–V; P–V; Capacitor load technique; PV cell; Temperature; Solar irradiance.

I. INTRODUCTION

Recently, the expansion of sustainable and renewable energy has advanced as a supplier of environmentally friendly electricity to solve problems including the shortage of fossil fuels, contamination, global warming, and other difficulties [1–5]. Our world obviously needs electrical power. The generation of electricity will progressively depend on alternative energy sources. In this regard, photovoltaic systems are widely used nowadays (solar power plants have steadily increased over the past 10 to 15 years) [6].

The matter of energy is a major one right now. Using renewable energy sources is a potentially beneficial solution to this issue. As a result, there is a significant amount of study and innovation being done in the sector of sustainable energy resources, including solar, thermal, wind, and ocean. However, the fact that solar energy may be employed to operate a variety of equipment draws a significant amount of interest. It is also an environmentally friendly form of energy. For the conversion of sunlight into electricity, solar photovoltaic cells and panels are employed. The most trustworthy information on a solar cell's efficiency at transforming sunlight into electricity is provided by its IV properties [7]. The most practical and extensively used way of directly generating electricity from sunlight for solar energy production is photovoltaic (PV) power generation, which may be used in both home and business settings [8–11]. The electrical performance of photovoltaic (PV) cells or arrays is greatly influenced by the ambient temperature and the solar radiation intensity (irradiation) as well. Thus, it is of utmost importance to acquire a quick and accurate measurement method of the voltage-current characteristic curve (I-V curve) of photovoltaic cells or arrays. Thus, from such an I-V curve, it was likely to calculate and evaluate the influence of radiation level and air temperature on the efficiency of PV systems [12-14].

It is widely recognized that when temperature rises, the efficiency of solar cells declines, principally because higher carrier concentrations cause the carrier internal recombination rate to increase [15]. In a photovoltaic (PV) system, the operating temperature has a linear relationship with both the energy conversion efficiency η and the output power P [16].

The regulation of the current provided by the photovoltaic panels between the zero-current point (Voc) and the short-circuit point (Isc) is the fundamental idea behind assessing the I-V curve. There are several ways to finish this job [17].

Controlling the current produced by the solar cells or modules between the zero-current point (Voc) and the short-circuit point (Isc) is the basic notion underlying assessing the I-V curve [18, 19]. The I-V curve of solar photovoltaic modules can be measured in many ways, such as with variable resistors, electronic loads, capacitive loads, bipolar power configurations, and four-quadrant power supplies [20, 22].

II. CHARACTERISTICS OF SOLAR CELL AND PV MODULES

A. Single diode model

A Solar module could be simulated as a diode in parallel with a current source. It is widely acknowledged that the circuit in Fig. 1 can serve as a model for a PV cell, having one [23, 24], two [25, 26] and, uncommonly, three or more diodes [27, 28]. Using single diode model, Fig. 1 illustrates the corresponding circuit for a solar cell [28]. A PV cell's single-diode equivalent circuit is composed of an irradiance-dependent current source Iph shunted by Rsh and followed by a series resistor Rs.

Equation (1) could be utilized to represent the current-voltage characteristics of the photovoltaic cell [29]:

$$I = I_{ph} - I_0[\exp\{\frac{q(V + I\,Rs)}{nkT}\} - 1] - (\frac{V + IRs}{Rsh}) \qquad (1)$$

where T is the cell temperature, q is the electronic charge, n is the diode ideality factor, and k is the Boltzmann constant. I represents the solar cell's output current, and V represents its output voltage, I_0 is the reverse saturation current, and I_{ph} is the photogenerated current.

B. Typical Fundamental characteristics

The usual I-V and P-V profiles of a photovoltaic module are shown in Fig. 2 (a) and (b), respectively. The short-circuit point Isc, open-circuit point Voc, and maximum power point Pmax are marked on the I-V/P-V curves. These three points are then used to determine Vmp, Imp, and Pmax.

The solar cell's efficiency (η) and fill factor (FF) are then determined using the equations (2, 3) [30]:

$$FF = \frac{Pmax}{Voc \times Isc} = \frac{Vmp \times Imp}{Voc \times Isc} \qquad (2)$$

$$\eta = \frac{Pmax}{Pin} = \frac{Isc \times Voc \times FF}{Pin} \qquad (3)$$

Where, P_{in} is the input optical power.

III. CAPACITIVE LOAD METHOD

The only way to accurately determine the electrical characteristics of a photovoltaic device is by experimental measurement of the I-V curve. The data provided by this measurement is extremely pertinent for the design, installation, and upkeep of PV systems. The regulation of the current supplied by the solar module between the zero-current point (Voc) and the short-circuit point (Isc) is the fundamental idea behind measuring the I-V curve. There are various ways to carry out this task, such as variable resistor, capacitive load, electronic load, bipolar power amplifier, four-quadrant power supply, and DC-DC converter [31].

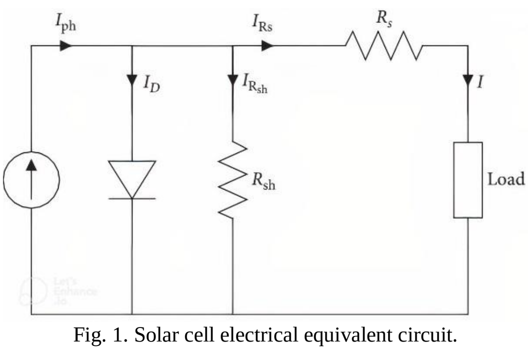

Fig. 1. Solar cell electrical equivalent circuit.

The SPV module's electrical curves are obtained using a capacitive loading approach, which is a common technique for all commercially available outdoor test facilities. Similar to a capacitor, the reactive component provides a low resistance path while it is being charged and an infinite resistance path after the capacitor voltage reaches the DC input voltage generated by the SPV module. The capacitor's auto-sweep capability enables minimal voltage and current ripple when the capacitor is used as a load to automatically and precisely sweep the electrical curve from Isc to Voc [32].

The capacitor simulates the characteristic as a variable resistor in this technique. The capacitor charge grows when the output DC voltage of the PV cell is introduced, the voltage progressively increases, and the current falls [33, 34]. Fig. 3 depicts the concept of that method [35].

The Photovoltaic module's terminals are connected directly to the capacitive load C via the S1 switch till the current I surpasses the open-circuit voltage Voc and data points are recorded for the characteristic curve because the capacitor's terminal voltage does not shift abruptly but instead starts growing gradually as the charge rises [36].

Throughout the capacitor charging period, an automatic rapid sweep of the I-V output curve from Isc to Voc is possible. After the measurements are finished, the capacitor's charge is discharged using a resistor linked to C via the switch S2 (with S1 open). Using the photovoltaic cell's single-diode similar circuit model from Fig. 2, a suitable capacitor's value C is calculated from [37]:

$$C = \frac{ts\ Isc}{2\ Voc} \qquad (4)$$

Where t_S is the sweep time (scan time), that is the time needed for the current I to charge C starting from I_{sc} until it decreases

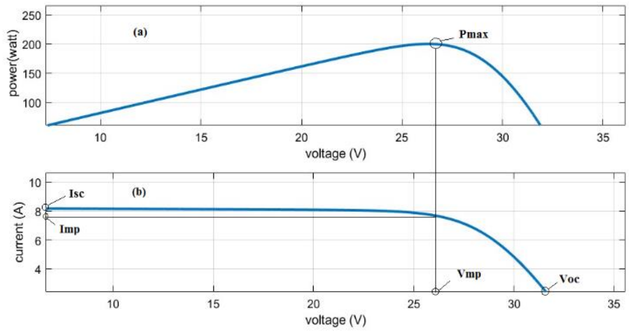

Fig. 2. (a) A conventional P-V curve showing the Maximum Power Point . (b) Vmp and Imp on the I-V curve are derived from the point Pmax on the P-V curve and also the fundamental parameters Isc and Voc are shown.

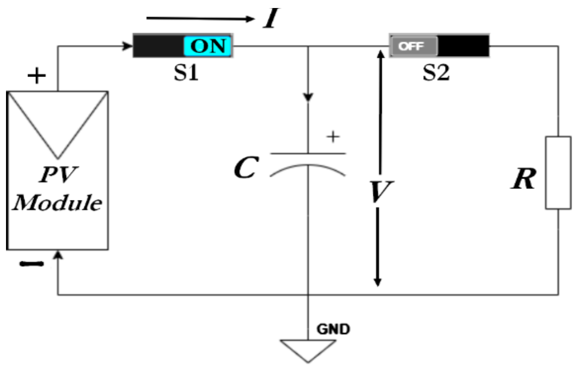

Fig. 3. Charging the capacitor C during the sweep phase of the I-V curve.

to the reverse saturation current I_0 of the diode's equivalent circuit. When the output PV voltage hits Voc and the current falls to I0 (almost zero), the charging ceases. The voltage climbs up from zero to the open-circuit voltage Voc in a period of time (t_S).

From (4), When choosing the size of the capacitor, the short circuit current to open circuit voltage ratio matters more than the photovoltaic system power. The "transient I-V curve" could be very well approximated by the I-V curve derived by steady state techniques by determining the minimal scan time (using constant resistive loads). Usually, t_S ranges from a few milliseconds to few seconds [38, 39].

III Numerical Validation

A. *Matlab Simulink Modeling Platform*

The most widely available I-V curve tracers use this technique [40, 41]. This highlights its relevance in practice, particularly for low and high-power PV systems, making this technique adaptable. It is important to stress that the technique gives a high level of adaptability to altering irradiation situations and under partial shading conditions (PSC), thus making the measurements of Isc and Voc with minimum error and ripple [42]. The parameters used in the schematic diagram of capacitive load method in Fig. 4 are the basic elements which are the PV array (Kyocera solar KC130GT), temperature sensor, and irradiation sensor.

The main circuit of the capacitive load method as shown in Fig. 5 consists of sensors (current measurement sensor and voltage measurement sensor), ultracapacitor load, and discharge resistor. A portable Digital Multimeter (DMM) with high voltage measurement capacity is typically required for measuring SPV output DC voltage. The DC output current of the SPV module can be measured using a variety of current sensors, including small shunt resistors, the ADS712, and DC current transducers made by LEM [43, 44].

When charging, the reactive component, which functions like a capacitor, gives a low resistance path; but, once the capacitor voltage reaches the DC input voltage generated by the SPV module, the reactive component offers an infinite resistance path. Capacitors come in a variety of varieties, but they might vary based on the task that needs to be done [44].

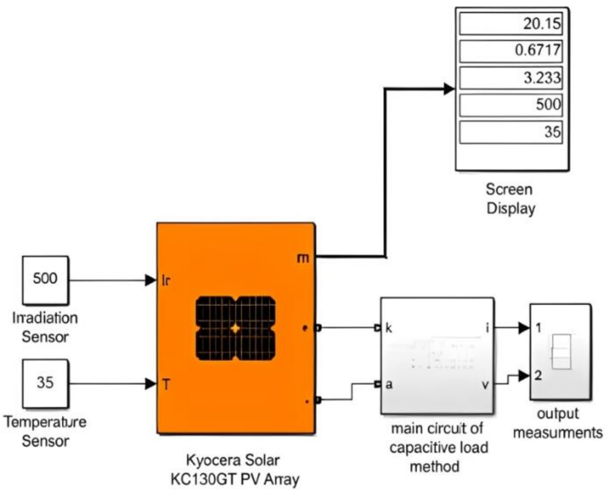

Fig. 4. The schematic diagram of capacitor load method.

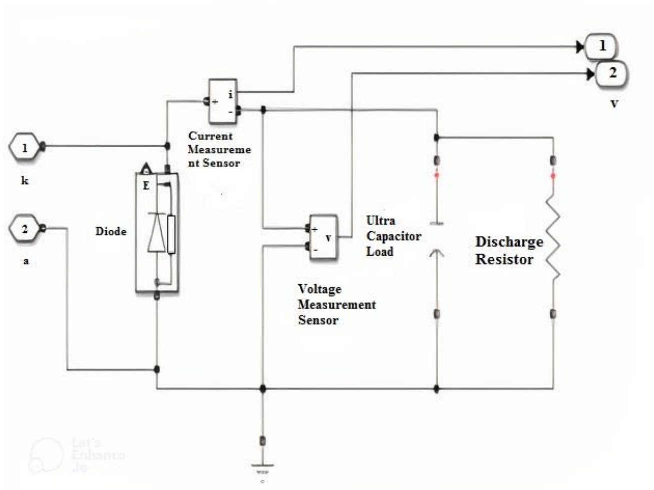

Fig. 5. Sub system 1 (main circuit of capacitive load method) in Fig. 4.

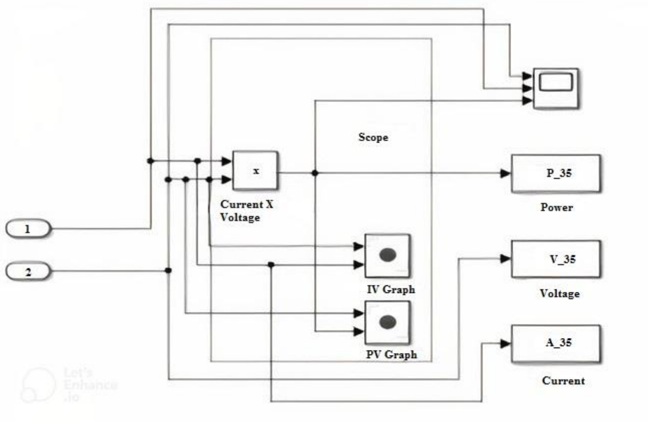

Fig. 6. Sub system 2 (output measurment) in Fig. 4.

MATLAB-based Simulink simulations are performed to scan the I-V curve of a polycrystalline solar array with 130W. Its commercial name is Kyocera solar KC130GT, and it has a maximum power of 130.064 watts and 36 cells per module as shown in TABLE I. Each string in the array has one module that is connected in parallel and one that is connected in series [45, 46].

For that PV cell, a MATLAB code has been implemented via the available toolboxes in the MATLAB package to get the P-V and I-V curves under various conditions of radiation intensity and temperature. In this paper, MATLAB (R2021b) is used to investigate the results and curves.

TABLE I. Electrical parameters of poly-crystal silicon PV module (Kyocera solar KC130GT)

Parameter	Value
Maximum Power (W)	130.064
Cells per module (Ncell)	36
Open circuit voltage V_{oc} (V)	21.9
Short-circuit current I_{sc} (A)	8.02
Voltage at maximum power point Vmp (V)	17.6
Current at maximum power point Imp (A)	7.39
Temperature coefficient of V_{oc} (%/deg.C)	-0.355
Temperature coefficient of I_{sc} (%/deg.C)	0.06
Shunt resistance R_{sh} (ohms)	63.1068
Series resistance R_s (ohms)	0.22103

B. *Irradiance and Temperature Effects on Electrical characteristics of PV module*

The influence of solar irradiance on the electrical properties of PV modules is modelled at constant temperatures of 25°C and solar irradiances of 250 W/m^2, 500 W/m^2, 750W/m^2 and 1000 W/m^2 and the modelling outcomes are shown in TABLE II. The P-V and I-V curves for the PV system are illustrated in Fig. 7 (a) and (b) respectively.

Under constant solar irradiation of 1000 W/m^2, the impact of temperature on the electrical properties of PV modules at 30, 35, 40, and 45°C is modeled and the results are shown in TABLE III. The PV module power-voltage (P-V) and current-voltage (I-V) curves are shown in Fig. 8 (a) and (b) respectively.

TABLE II. The PV module characteristics with 250, 500, 750, and 1000 W/m^2 of solar radiation at 25°C of constant temperature

Electrical Characteristics	**Solar irradiance (W/m^2)**			
	250	**500**	**750**	**1000**
Isc(A)	2.020	4.041	6.061	8.081
Voc (V)	20.12	20.94	21.36	21.65
Pmax (W)	32.22	65.5928	97.9572	136.5336
Vm	18	18.02	18.04	18.06
Im	1.79	3.64	5.43	7.56
FF	0.7928	0.7752	0.7566	0.7804
η (%) at 25°C	13.8715	14.1196	14.0576	14.6953

TABLE III. The PV module characteristics with 30, 35, 40, and 45°C of temperature at 1000 W/m^2 of constant radiation.

Electrical Characteristics	**Temperature (°C)**			
	30	**35**	**40**	**45**
Isc(A)	8.105	8.129	8.154	8.178
Voc (V)	21.27	20.88	20.49	20.11
Pmax (W)	125.85	123.98	121.53	118.77
Vm	17.75	17.10	16.58	16.05
Im	7.09	7.25	7.33	7.40
FF	0.7300	0.7304	0.7274	0.7222
η (%) at 1000 w/m^2	13.5454%	13.3441%	13.0804%	12.7833%

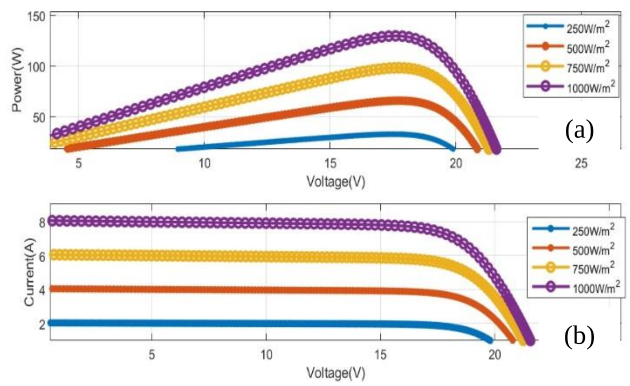

Fig. 7 (a) I-V curves at different radiation and constant temperature (25 °C). (b) The corresponding P-V curves.

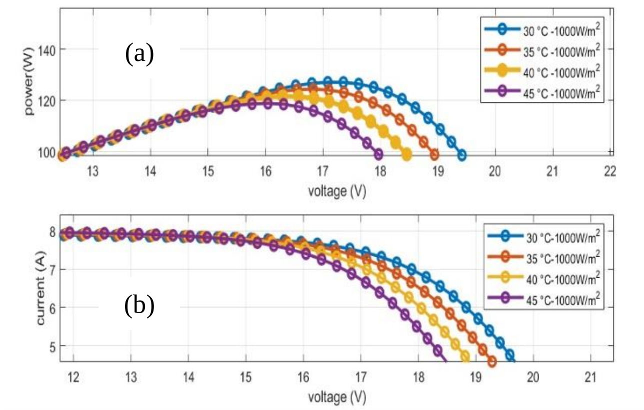

Fig. 8 (a) I-V curves at different Temperatures and constant Irradiance (1000w/m^2). (b) The corresponding P-V curves.

C. *The Relation of the Electrical Parameters*

It is possible to explain these relationships more accurately and graphically by studying the inter-relationships between the PV cell parameters at variable irradiance or temperature [47]. The parameters will be illustrated, such as (Voc, Isc, FF, and efficiency η).

First, the relationship at specific temperature between solar irradiation, Isc (short circuit current), and Voc (open circuit voltage). At a temperature of 25°C, the Irradiance values are 250, 500, 750, and 1000 w/m^2. As shown in Fig. 9, it has been discovered that the open circuit voltage Voc and the short circuit current Isc both rise with irradiation [48].

The effect of irradiance at constant temperature on the efficiency (η) and the fill factor (FF) is shown in Fig. 10. As the irradiance increases at constant temperature (25°C), the efficiency of the cell will increase to reach 14.7% at 1000 W/m^2.

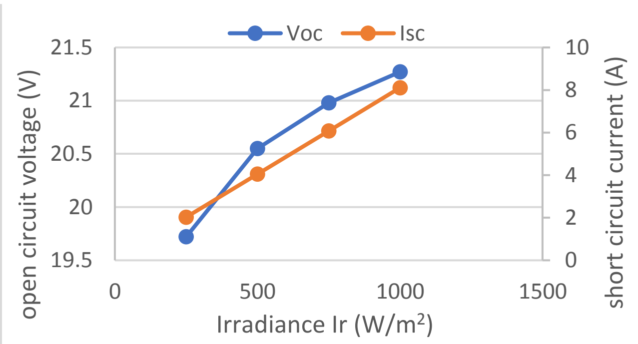

Fig. 9. Open-circuit voltage (Voc) and short-circuit current (Isc) for a polycrystalline silicon solar cell as function of irradiance at constant tempraeture (25°C).

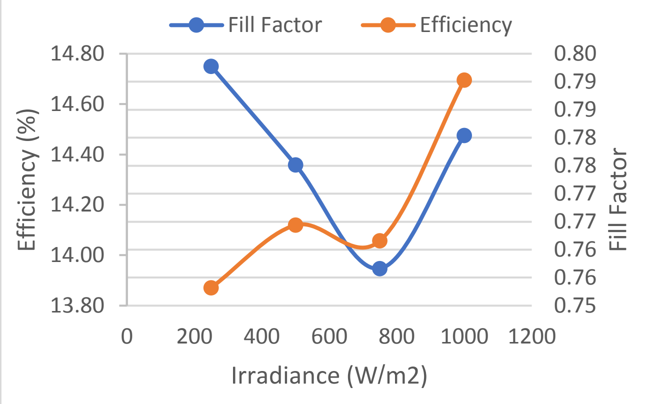

Fig. 10. The efficiency (η) and the fill factor (FF) for a polycrystalline silicon solar cell as a function of irradiance at constant tempreature (25°C).

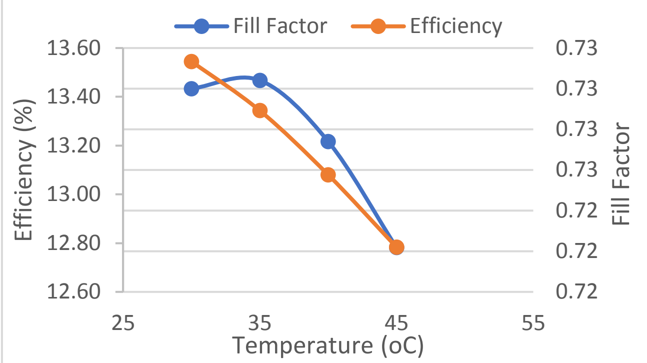

Fig. 12. The efficiency (η) and the fill factor (FF) for a polycrystalline silicon solar cell as a function of tempreature at constant irradiance (1000w/m^2).

Regarding the variation with temperature, it is well known that, most of the characteristics of semiconductor materials are impacted by a semiconductor's bandgap, which is reduced as temperature rises [49]. Fig. 11 shows that Voc decreases with temperature (at constant Irradiance=1000W/m^2). This is attributed to the excess rise in the reverse saturation current compared to the photogenerated current. However, Isc does somewhat rise with temperature because the bandgap energy, E_G, drops with temperature, allowing more photons to have sufficient energy to form electron-hole pairs. However, this is a tiny effect. Its relative increase is of the order of 0.06% per °C for silicon [50].

Concerning the effect of temperature on the efficiency (η) and the fill factor (FF), it is revealed in Fig. 12, that η decreases with increasing temperature, at constant Ir (1000 w/m^2). The efficiency drops to 12.8% at 45ºC. Its relative decrease is of the order of -0.15% per ºC [51]. But the fill factor at low temperature less than 35°C increases, and subsequently decreases with increasing temperature.

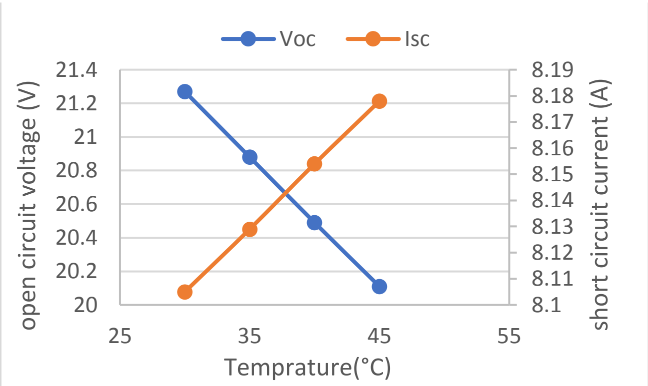

Fig. 11. Open-circuit voltage (Voc) and short-circuit current (Isc) for a polycrystalline silicon solar cell as a function of tempreature at constant irradiance (1000W/m^2).

IV. Conclusion

In this paper, the performance of PV cells was examined in relation to temperature and irradiance. Two scenarios were used to conduct this investigation. The first involved investigating how the primary characteristics of a poly-crystal silicon PV module were affected by varying irradiance at a constant temperature. The second focused on the impact of varying temperature while maintaining irradiance. The capacitive load method was used to identify and extract the key parameters. The outcomes showed that irradiance will enhance the performance of the PV cell by raising its efficiency to 14.7% at 1000 W/m^2 at constant temperature (25ºC). When considering how temperature affects PV cell efficiency, it is found that, under constant irradiance (1000 w/m^2), decreases with increasing temperature. At 45ºC, the efficiency falls to 12.8%. The researcher recommends an investigation of the effect of series and parallel connection with temperature and irradiance on the PV cell efficiency as a future work.

REFERENCES

[1] H. E. Murdock, D. Gibb, T. AndrØ, J. L. Sawin, A. Brown, F. Appavou, G. Ellis, B. Epp, F. Guerra, and F. Joubert, ‘"Renewables 2020-global status report,’" Global Trends Renew. Energy Investment, Frankfurt School-UNEP Collaborating Centre Climate Sustain. Energy Finance, BloombergNEF, UN Environ. Programme, Paris, France, Tech. Rep. REN21, 2020. Available: https://www.ren21.net/wpcontent/uploads/2019/05/gsr_2020_full_report_en.pdf

[2] G. P. Peters, R. M. Andrew, J. G. Canadell, P. Friedlingstein, R. B. Jackson, J. I. Korsbakken, C. Le QuØrØ, and A. Peregon, "Carbon dioxide emissions continue to grow amidst slowly emerging climate policies," Nature Climate Change, Vol. 10, No. 1, pp. 3–6, Jan. 2020.

[3] J. G. J. Olivier and J. A. H. W. Peters, "Trends in global Co2 and total greenhouse gas emissions: 2020 report," in PBL Netherlands Environment. The Hague, The Netherlands: Assessment Agency, 2020.

[4] M. A. Aktar, M. M. Alam, and A. Q. Al-Amin, "Global economic crisis, energy use, CO2 emissions, and policy roadmap amid COVID-19," Sustain. Prod. Consumption, Vol. 26, pp. 770–781, Apr. 2021.

[5] J. Sayyad and P. Nasikkar, "Solar photovoltaic performance monitoring: A bibliometric review, research gaps and opportunities," Library Philosophy Pract. (e-J.), pp. 1–25, Dec. 2020. Available: https://digitalcommons.unl.edu/libphilprac/4830/

[6] R. Pal, V. K. Sethi, and A. Gour, "Assessing the Performance of 100 kW Solar PV Power-plants Through I-V Characterization & Validation of Tilted Irradiance Calculation Compared to an Hourly Model," International Research Journal of Engineering and Applied Science, Vol. 2, No. 1, Mar. 2014

[7] V.A. Pilipovich, S.A. Sergienya, A.K. Esman and V.B. Zalesskii, "An automated system for measuring the current-voltage charasteristics of solar cells", Measurement Techniques, Vol. 48, No. 6, 2005

[8] C. Reise, B. Müller, D. Moser, G. Belluardo, and P. Ingenhoven, "Uncertainties in PV system yield predictions and assessments," Int.Energy Agency, Paris, France, Tech. Rep. IEA-PVPS T13-12, 2018. Available: https://iea-pvps.org/wp-content/uploads/2020/01/Uncertainties_in_PV_System_Yield_Predictions_and_Assessments_by_Task_13.pdf

[9] R. Srivastava, A. N. Tiwari, and V. K. Giri, "An overview on performance of PV plants commissioned at different places in the world," Energy Sustain. Develop., Vol. 54, pp. 51–59, Feb. 2020.

[10] IRENA, "Future of Solar Photovoltaic: Deployment, Investment, Technology, Grid Integration, and Socio-Economic Aspects," International Renewable Energy Agency, Abu Dhabi, United Arab Emirates, 2019.

[11] B. S. Kumar and K. Sudhakar, "Performance evaluation of 10 MW grid connected solar photovoltaic power plant in India," Energy Rep., Vol. 1, pp. 184–192, Nov. 2015.

[12] V. Leite, J. Batista, F. Chenlo, and J. L. Afonso, "Low-cost instrument for tracing I-V characteristics of photovoltaic modules," in Proc. Int.Conf. Renew. Energies Power Qual. (ICREPQ), Santiago de Compostela, Spain, Vol. 1, No. 10, pp. 1012–1017, Mar./Apr. 2012. Available: https://www.icrepq.com/icrepq'12/565-leite.pdf

[13] V. Leite and F. Chenlo, "An improved electronic circuit for tracing the IV characteristics of photovoltaic modules and strings," in Proc. Int.Conf. Renew. Energies Power Qual. (ICREPQ), Vol. 1, No. 8, pp. 1224–1228, Apr. 2010. Available: https://icrepq.com/icrepq'10/629-Leite.pdf

[14] R. E. Campos, E. Y. Sako, H. S. Moreira, J. L. de Souza Silva, and M. G. Villalva, "Experimental analysis of a developed I-V curve tracer under partially shading conditions," in Proc. IEEE PES Innov. Smart Grid Technol. Conf.-Latin Amer. (ISGT Latin Amer.), pp. 1–5, Sep. 2019.

[15] A. Rezky, K. Devara, N. S. Wardana, S. Ramadhanty, and T. Abuzairi, "Simple method for I-V characterization curve for low power solar cell using arduino nano," E3S Web of Conferences, Vol. 67, No. 01020, 2018.

[16] E. Durán, M. Piliougine, M. Sidrach-de-Cardona, J. Galán, and J.M. Andújar, "Different Methods to Obtain the I-V Curve of PV Modules: A Review," 33rd IEEE Photovoltaic Specialists Conference, pp. 1-6, 2008.

[17] I. F. Silva, P. S. Vicente, F. L. Tofoli, and E. M. Vicente, "Portable and low cost photovoltaic curve tracer," in Proc. Brazilian Power Electron. Conf. (COBEP), pp. 1–6, Nov. 2017.

[18] V.A. Pilipovich, S.A. Sergienya, A.K. Esman and V.B. Zalesskii, "An automated system for measuring the current-voltage charasteristics of solar cells," Measurement Techniques, Vol. 48, No.6, 2005.

[19] M.A. Green, A.W. Blakers, and C.R. Osterwald "Characterization of high-efficiency silicon solar cells," J. Appl Phys, Vol. 58, No. 11, pp. 4402–4408, 1985.

[20] P. Papageorgas, D. Piromalis, K. Antonakoglou, G. Vokas, D. Tseles, and K.G. Arvanitis, "Smart solar panels: In-situ monitoring of photovoltaic panels based on wired and wireless sensor networks," Energy Procedia, Vol. 36, pp. 535–545, 2013.

[21] A. Vega, V. Valiæo, E. Conde, A. Ramos, and P. Reina, "Double sweep tracer for I-V curves characterization and continuous monitoring of photovoltaic facilities," Sol. Energy, Vol. 190, pp. 622–629, Sep. 2019.

[22] V. Leite, J. Batista, F. Chenlo, and J. L. Afonso, "Low-cost I-V tracer for photovoltaic modules and strings," in Proc. Int. Symp. Power Electron., Electr. Drives, Autom. Motion, pp. 971–976, Jun. 2014.

[23] M.A. Green. "Solar cell fill factors: General graph and empirical expressions," Solid State Electron, Vol. 24, No. 8, pp. 788–789, 1981.

[24] J. Aller, J. Viola, F. Quizhpi, J. Restrepo, A. Ginart, and A. Salazar. "Implicit PV cell parameters estimation used in approximated closed-form model for inverter power control," In Proceedings of the 2017 IEEE Workshop on Power Electronics and Power Quality Applications (PEPQA), Bogotá, Colombia, pp. 1–6, 31 May–2 June 2017.

[25] D. Chan, and J. Phang. "Analytical Methods for the Extraction of Solar-Cell Single- and Double-Diode Model Parameters from I-V Characteristics," IEEE Trans. Electron Devices, Vol. 34, No. 2, pp. 286-293, Feb. 1987.

[26] K. Ishaque, and Z. Salam. "A comprehensive MATLAB Simulink PV system simulator with partial shading capability based on two-diode model," Sol. Energy, Vol. 85, No. 9, pp. 2217-2227, 2011.

[27] J.J. Soon, K.S. Low, and S.T. Goh. "Multi-dimension diode photovoltaic (PV) model for different PV cell technologies," In Proceedings of the IEEE 23rd International Symposium on Industrial Electronics (ISIE), Istanbul, Turkey, pp. 1–6, 1–4 June 2014.

[28] P.K. Pandey, and K.S. Sandhu. "Multi Diode Modelling of PV Cell," In Proceedings of the IEEE 6th India International Conference on Power Electronics (IICPE), Kurukshetra, India, pp. 1–4, 8–10 December 2014.

[29] J.M. Álvarez, D. Alfonso- Corcuera, E. Roibás-Millán, J. Cubas, J. Cubero-Estalrrich, A. Gonzalez-Estrada, R. Jado-Puente, M. Sanabria-Pinzón, ans S. Pindado, "Analytical Modeling of Current-Voltage Photovoltaic Performance: An Easy Approach to Solar Panel Behavior, Appl. Sci., Vol. 11, No. 4250, 2021.

[30] A.D.Hansen, P. E.Sørensen, L. H.Hansen, and H.W.Bindner, Models for a stand-alone PV system. Forskningscenter, 1219, 2001.

[31] E. Durán, M. Piliougine, M. Sidrach-de-Cardona, J. Galán, and J.M. Andújar, "Different methods to obtian the I-V curve of PV modules: A review," in Conference Record of the IEEE Photovoltaic Specialists Conference · May 2008.

[32] F. Spertino, J. Ahmad, A. Ciocia, P. Di Leo, A.F. Murtaza, M. Chiaberge, "Capacitor charging method for I–V curve tracer and MPPT in photovoltaic systems," Sol. Energy, 119, 461–473, 2015.

[33] F. Spertino, J. Ahmad, P. Di Leo, and A. Ciocia, "A method for obtaining the I-V curve of photovoltaic arrays from module voltages and its applications for MPP tracking," Sol. Energy, Vol. 139, pp. 489–505, Dec. 2016.

[34] Y. Erkaya, P. Moses, and S. Marsillac, "On-site characterization of PV modules using a portable, MOSFET-based capacitive load," in Proc. IEEE 43rd Photovoltaic Spec. Conf. (PVSC), pp. 3119–3122, Jun. 2016.

[35] J. Sayyad, P. Nasikkar, A.P. Singh, S. Ozana, "CapacitiveLoad-Based Smart OTF for HighPower Rated SPV Module," Energies, Vol. 14, No. 788, 2021.

[36] K. V. G. Raghavendra, K. Zeb, A. Muthusamy, T. Krishna, S. Kumar, D.-H. Kim, M.-S. Kim, H.-G. Cho, and H.-J. Kim, "A comprehensive review of DC–DC converter topologies and modulation strategies with recent advances in solar photovoltaic systems," Electronics, Vol. 9, No. 1, pp. 31, 2020.

[37] M.M. Mahmoud, "Transient analysis of a PV power generator charging a capacitor for measurement of the I–V characteristics,Renewable Energy", Vol. 31, No. 13, pp. 2198-2206, 2006.

[38] S. Gaiotto, A. Laudani, F. R. Fulginei, and A. Salvini, "An advanced measurement equipment for the tracing of photovoltaic panel I–V curves," in Proc. Int. Conf. Renew. Energy Res. Appl. (ICRERA), pp. 1010–1014, Nov. 2015.

[39] E. Matic, J. Marko, and T. Marko. "Optimal I-V Curve Scan Time of Solar Cells and Modules in Light of Irradiance Level," International Journal of Photoenergy, Vol. 2012, No. 151452, pp. 1-11, 2012.

[40] J. Sayyad and P. Nasikkar, "Design and Development of Low Cost, Portable, On-Field I-V Curve Tracer Based on Capacitor Loading for High Power Rated Solar Photovoltaic Modules," in IEEE Access, Vol. 9, pp. 70715-70731, 2021.

[41] A. Sahbel, N. Hassan, M. M. Abdelhameed, and A. Zekry, "Experimental performance characterization of photovoltaic modules using DAQ," Energy Procedia, Vol. 36, pp. 323–332, 2013.

[42] F. Spertino, J. Sumaili, H. Andrei, and G. Chicco, "PV module parameter characterization from the transient charge of an external capacitor," IEEE J. Photovolt., Vol. 3, No. 4, pp. 1325–1333, Oct. 2013.

[43] S. Singer, "The application of loss-free resistors in power processing circuits," IEEE Trans. Power Electron., Vol. 6, No. 4, pp. 595–600, Oct. 1991.

[44] J. Sayyad, P. Nasikkar, A.P. Singh, and S. Ozana. "Capacitive Load-Based Smart OTF for High Power Rated SPV Module," Energies, Vol. 14, No. 788, 2021.

[45] A.Q. Malik, and S.J. Damit, "Outdoor testing of single crystal silicon solar cells", Renewable Energy, Vol. 28, pp.1433-1445, 2003.

[46] E. V. Dyk, A. Gxasheka, and E. Meyer, "Monitoring current–voltage characteristics and energy output of silicon photovoltaic modules," Renew. Energy, Vol. 30, No. 3, pp. 399–411, 2005.

[47] S. Das. "Development of a Low-cost, Portable, and Programmable Solar Module to Facilitate Hands-on Experiments and Improve Student Learning," Faculty Publications, 2016

[48] I. Daut, M. Sembiring, M. Irwanto, N. Syafawati, and S. Hasan. "Hargreaves Model For Estimating Solar Radiation in Perlis," International Conference: Electrical Energy and Industrial Electronic Systems EEIES 2009, Penang, Malaysia, 7-8 December 2009.

[49] M.J. Wu, E. J. Timpson and S. E. Watkins, "Temperature considerations in solar arrays," Region 5 Conference: Annual Technical and Leadership Workshop, pp. 1-9, 2004.

[50] A. B. Sproul and Green, M. A., "Improved value for the silicon intrinsic carrier concentration from 275 to 375 K," Journal of Applied Physics, vol. 70, pp. 846-854, 1991.

[51] D. M. Fébba, R. M. Rubinger, A. F. Oliveira, and E. C. Bortoni. "Impacts of temperature and irradiance on polycrystalline silicon solar cells parameters," Solar Energy, Vol. 174, pp. 628-639, 2018.